METHODS

A three-dimensional axis for the study of femoral neck orientation

Noémie Bonneau,[1] Paul-Antoine Libourel,[2] Caroline Simonis,[3] Laurent Puymerail,[4,5] Michel Baylac,[6] Christine Tardieu[1] and Olivier Gagey[7,8]

[1]UMR 7179 CNRS-Muséum National d'Histoire Naturelle, Paris Cedex, France
[2]UMR 5167 CNRS-Université Claude Bernard-Institut Fédératif des Neurosciences de Lyon, Lyon Cedex, France
[3]Ministère de l'Éducation Nationale, DEPP, Paris, France
[4]UMR 7268 CNRS-Université d'Aix-Marseille-EFS, Marseille Cedex, France
[5]UMR 7194 CNRS-Muséum National d'Histoire Naturelle, Paris Cedex, France
[6]UMR 7205 CNRS-Muséum National d'Histoire Naturelle, Paris Cedex, France
[7]Bicêtre University Hospital, AP-HP, Paris, France
[8]JE 2494 University Paris-Sud Orsay, Paris, France

Abstract

A common problem in the quantification of the orientation of the femoral neck is the difficulty to determine its true axis; however, this axis is typically estimated visually only. Moreover, the orientation of the femoral neck is commonly analysed using angles that are dependent on anatomical planes of reference and only quantify the orientation in two dimensions. The purpose of this study is to establish a method to determine the three-dimensional orientation of the femoral neck using a three-dimensional model. An accurate determination of the femoral neck axis requires a reconsideration of the complex architecture of the proximal femur. The morphology of the femoral neck results from both the medial and arcuate trabecular systems, and the asymmetry of the cortical bone. Given these considerations, two alternative models, in addition to the cylindrical one frequently assumed, were tested. The surface geometry of the femoral neck was subsequently used to fit one cylinder, two cylinders and successive cross-sectional ellipses. The model based on successive ellipses provided a significantly smaller average deviation than the two other models ($P < 0.001$) and reduced the observer-induced measurement error. Comparisons with traditional measurements and analyses on a sample of 91 femora were also performed to assess the validity of the model based on successive ellipses. This study provides a semi-automatic and accurate method for the determination of the functional three-dimensional femoral neck orientation avoiding the use of a reference plane. This innovative method has important implications for future studies that aim to document and understand the change in the orientation of the femoral neck associated with the acquisition of a bipedal gait in humans. Moreover, the precise determination of the three-dimensional orientation has implications in current research involved in developing clinical applications in diagnosis, hip surgery and rehabilitation.

Key words: anteversion; biomechanics; biomedical engineering; bipedal gait; femur; neck–shaft angle.

Introduction

The femoral neck is well developed in humans, with a global orientation slanting upwards and forwards (Kapandji,

2007; Klein & Sommerfeld, 2008; Fig. 1A). As the femoral neck is subjected to important biomechanical constraints, especially during the one-legged stance of the walking cycle, a proper three-dimensional orientation is key to ensure an economic bipedal gait and posture. Abnormality in this orientation may be associated with problems in the loading of the hip joint, which may result in non-economic gait and premature wear of the joint (Siffert, 1981; Reikeras & Hoiseth, 1982; Wedge et al. 1989; Tönnis & Heinecke, 1999). Consequently, an accurate determination of the orientation of the femoral neck has important implications.
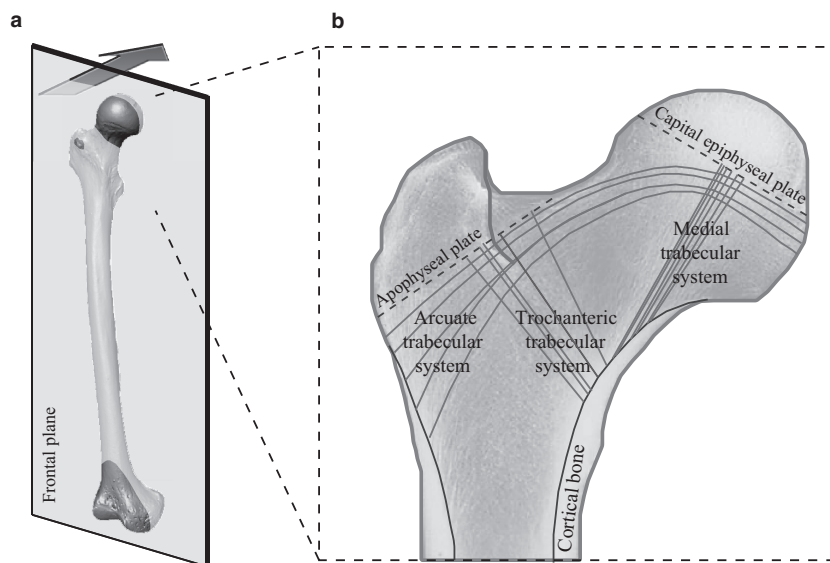
Fig. 1 (A) The femoral neck is well developed in *Homo sapiens*, with a global orientation slanting upwards and forwards. (B) The proximal femur presents a complex three-dimensional architecture. The cortical bone presents an asymmetric cross-sectional distribution along the femoral neck: a thick cortex is observed in the inferior part, while the cortex in the superior part is thin. The trabecular bone is organised along three major trabecular systems – medial, trochanteric and arcuate – surrounding an area of less resistance named Ward's triangle.

Traditionally, the orientation of the femoral neck is quantified using angles such as the angle of anteversion and the neck–shaft angle. These angles describe the orientation only in a few planes (generally in two planes) rather than in three dimensions. With the rapid development of medical three-dimensional imaging, it becomes increasingly important to use accurate three-dimensional orientation of the femoral neck in order to obtain more informative data. The precise determination of the three-dimensional orientation likely has implications in current research involved in developing clinical applications in diagnosis (e.g. congenital dislocation of the hip), hip surgery (e.g. computer-assisted total hip replacement surgery) and rehabilitation. Moreover, an accurate determination of the three-dimensional axis would advance biomechanics and modelling studies (e.g. finite element analysis). Improvements in biomechanical models have important evolutionary implications for documenting and understanding the changes in the orientation of the femoral neck associated with bipedal gait acquisition in the human lineage.

Regarding the large and old (Wolff, 1892) multidisciplinary literature on the femoral neck, a wide number of methods is available that revolve around the measurement of the traditional angles used to quantify the femoral neck orientation, i.e. the angle of anteversion and the neck–shaft angle. Methods by physical examinations on patients (e.g. Staheli et al. 1985; Ruwe et al. 1992) allow clinicians to obtain rapidly data on living humans, yet they are rather imprecise. Methods based on measurements using both anatomical femora (e.g. Durham, 1915; Kingsley & Olmsted, 1948; Yoshioka et al. 1987; Wedge et al. 1989; Tayton, 2007) and medical imaging, such as radiology (e.g. Rogers, 1931; Dunlap et al. 1953; Ryder & Crane, 1953; Rippstein, 1955; Magilligan, 1956; Haspl & Bilic, 1996), computed tomography (e.g. Murphy et al. 1987; Deghrar et al. 1997;

Strecker et al. 1997; Kim et al. 2000a,b; Delialioglu et al. 2006), magnetic resonance imaging (e.g. Tamari et al. 2005) and ultrasound (e.g. Moulton & Upadhyay, 1982; Braten et al. 1992) provide more precise measurements. Yet, despite the advances in 3D-imaging technology, measurements are frequently based on two-dimensional views. However, these views are known to depend on the orientation of the reference plane used to describe the position of the femur (Murphy et al. 1987; Kim et al. 2000a,b). Problems with the use of a reference plane are that, on the one hand, the variation of the landmarks used to compute this plane is ignored (Bookstein, 1991; Dryden & Mardia, 1998; Slice, 2005) and, on the other hand, the definition of this plane changes according to the material used, the method and/or the operator expertise resulting in different measurements. Most important is the frequent difficulty, pointed out by different authors, to determine the true femoral neck axis during measurements. Each author formulates different methods to acquire the neck axis, resulting in different results for a same individual. For example, some define the femoral neck axis as the middle between the proximal and the distal borders of the neck (Kingsley & Olmsted, 1948; Ruwe et al. 1992), while others used external landmarks, such as the centre of the femoral head or the shape of the greater trochanter (Yoshioka et al. 1987; Haspl & Bilic, 1996; Kim et al. 2000b). However, the centre of the femoral head is not necessarily always positioned on the axis of the neck (Kingsley & Olmsted, 1948), and it is known that the morphology of the greater trochanter depends on the variability in muscle attachment (Duda et al. 1996). Most often, a simple visual determination is used to determine the femoral neck axis. Thus, according to the method, measurements may result in different values despite the fact that each author obtained repeated measurements with low observer error. The

purpose of this study is to identify an accurate and semi-automatic method to determine the functional three-dimensional orientation of the femoral neck using a three-dimensional model (Kim et al. 2000b; Zebaze et al. 2005). This method should describe the proper orientation of the femoral neck in the full three-dimensional space and avoid problems due to the use of a reference plane.

Materials and methods

Material

The study included 50 specimens of modern *Homo sapiens*, resulting in a total sample of 91 femora (43 right and 48 left) of known age and sex. The sample was composed of 21 women and 29 men, with a mean age, respectively, of 45.9 years (SD = 17.7 years, range = 18–82 years) and 50.8 years (SD = 16.4 years, range = 20–87 years). These femora are part of the SIMON collection (housed at the University of Geneva, Switzerland) and of the collections of the National Museum of Natural History of Paris (MNHN, France). The SIMON collection is composed of skeletons dated from the 20th century and collected in cemeteries from Vaud (Perréard Lopreno & Eades, 2003). Femora housed in the collections of the MNHN correspond to French individuals from the 21th century.

Determination of the three-dimensional orientation of the femoral neck

The femur was immobilised in a clamp, and three-dimensional coordinates (*x*, *y*, *z*) were recorded in a millimetric orthonormal reference system using a MicroScribe® G2 (Immersion) with a precision of ± 0.38 mm according to the manufacturer. Using the stylus of the MicroScribe, programmed to take three-dimensional coordinates 1 mm apart, the exterior surface of the femoral neck was scanned, and between 900 and 1200 points were recorded. This digitised external contour records the general shape of the femoral neck, which can be influenced by the cortical bone morphology as well as the medial and arcuate trabecular systems, which have different

orientations. The raw point cloud was used in different regression approaches, where the fit was estimated based on the least-squares method.

The femoral neck can be considered as a circular cross-sectional cylinder as a first approximation (e.g. Rafferty, 1998; Seeman et al. 2001; Zebaze et al. 2005). Thus, the first regression was based on the equation of a circular cylinder (Fig. 2A). Based on the totality of the three-dimensional coordinates acquired on the femoral neck, a regression using the software GEOMAGIC STUDIO 10 (www.geomagic.com/) was performed. The orientation of the main axis was recorded as a first femoral neck axis.

However, a precise re-examination of the architecture of the proximal femur provides evidence that its structure is more complex (Fig. 1B). The cortical bone presents an asymmetric cross-sectional distribution: a thick cortex is observed in the inferior part of the femoral neck while the cortex in the superior part is thin (Lovejoy, 1988, 2005; Ohman et al. 1997; Rafferty, 1998; Matsumura et al. 2010). Moreover, the trabecular bone of the proximal part of the femur is organised along three major trabecular systems (medial, trochanteric and arcuate; Skuban et al. 2009) surrounding an area of less resistance named Ward's triangle. This complex three-dimensional architecture thus complicates the determination of the orientation of the femoral neck. Consequently, in addition to the simplistic model based on a circular cylinder, we here propose to test two alternative models that take into account the complexity of the architecture of the femoral neck.

To do so, a second model based on two cylinders was developed (Fig. 2B). The superior part of the femoral neck, composed of both a thin cortex and the arcuate trabecular system, presents a different orientation compared with the inferior part that is composed of both a thick cortex and the medial trabecular system. Thus, based on two cylinders, the two parts were modelled independently. The points of the inferior and superior parts of the femoral neck were selected and used separately to perform a regression based on the equation of a circular cylinder (GEOMAGIC STUDIO 10), resulting in a model with two cylinders. The mean orientation of the two cylinders corresponds to a second femoral neck axis.

Finally, a custom-designed function in MATLAB v.7.8.0 (www.mathworks.com/) was established to model the femoral neck based on successive cross-sectional ellipses (Fig. 2C). Indeed, an ellipse is defined by two foci, and this feature was exploited here to obtain
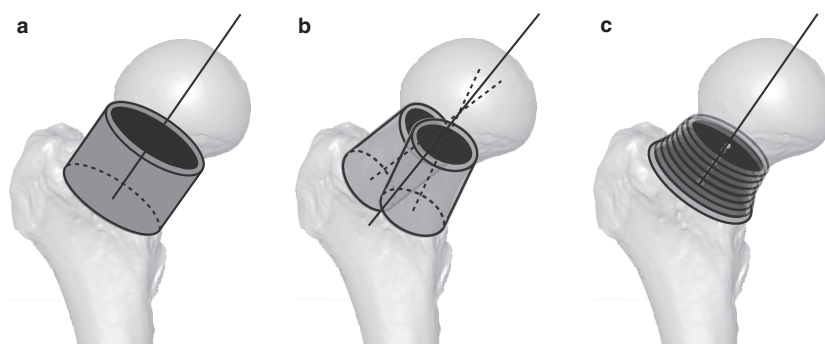
Fig. 2 Three three-dimensional models were tested to determine the three-dimensional orientation of the femoral neck. The most intuitive model was the one based on a single cylinder (A). The superior part of the femoral neck, composed of both a thin cortex and the arcuate trabecular system, presents a different orientation compared with the inferior part, which is composed of both a thick cortex and the medial trabecular system. Thus, based on two cylinders, the two parts were modelled independently (B). Finally, the femoral neck was modelled based on successive cross-sectional ellipses (C). An ellipse is defined by two foci, a feature that was exploited here to obtain, in a single object, the two orientations of the superior and inferior parts of the femoral neck.

in a single object the two orientations of the superior and inferior parts of the femoral neck. The axis of inertia of the total point cloud was calculated, providing a first axis to cut the cloud in equidistant cross-sections that are separately used to compute an elliptic regression. At the cross-sectional extremities of the point cloud, the points did not represent a complete ellipse and they were eliminated. Based on the centres of the successive ellipses, a principal component analysis (PCA) was performed, and the first principal component provided a new axis that was used to reiterate the process. The axis defined by the centres of the successive ellipses obtained in the second process is considered as a third femoral neck axis.

Comparison of the three models proposed to determine the femoral neck axis

All analyses were performed using the R graphical and statistical package v.2.9.0 (R Development Core Team, 2011). Comparisons between the three models were made using, first, the average deviation and, second, different measurement errors.

The average deviation was defined as the mean of the distances of each real point from the theoretical regression surface. It was computed for each model in a sub-sample of 25 individuals resulting in 50 femora (25 right and 25 left). For the model based on successive cross-sectional ellipses, all points of the point cloud were used in the calculation, i.e. as well as the points eliminated at the cross-sectional extremities because they did not represent a complete ellipse. An ANOVA (analysis of variance) was performed to compare the values of the average deviations obtained using the three different regressions.

The three-dimensional axes, obtained based on the three different regressions, were used to evaluate the method- and observer-induced measurement errors of each model. Six left femora were used in these tests. Several methods to assess measurement error in morphometrics have been described in the literature (see von Cramon-Taubadel et al. 2007 for a recent review). von Cramon-Taubadel et al. (2007) proposed a protocol based on a partial superimposition. Three reference landmarks, tested to be homologous landmarks with minimal variance, are used to superimpose the different repetitions performed on a specimen, and the measurement variance was computed on the non-reference homologous landmarks. In this study, the method- and observer-induced measurement errors were assessed using a variant of the protocol proposed by von Cramon-Taubadel et al. (2007). Five stainless-steel nails, with a diameter of 1 mm, were implanted in each of the six femora in order to generate a three-dimensional system of reference landmarks. The bone was pierced by means of a 0.9-mm-diameter drill, and stainless-steel nails were placed in the holes. Nails were implanted homogeneously in all the femora. Based on these nails, a partial superimposition, performed using a custom-designed function of the Rmorph library for R (Baylac, 2010), was used to reorient the successive acquisitions performed on a specimen. The superimposition process, based on a generalised Procrustes analysis (Gower, 1975; Rohlf & Slice, 1990), corresponds to a scaling step followed by translations and rigid three-dimensional rotations of the bones using the landmarks defined by the five nails. The three-dimensional coordinates acquired on the femoral neck surface and used to compute the axis of the femoral neck followed passively the translations and rotations calculated using the five nail coordinates. The use of nails to perform the partial superimposition guarantees a minimal variance of the measurement error of the reference landmarks

(mean = 0.52 mm; SD = 0.19 mm), whereas homologous landmarks acquisition is necessarily observer dependent. Moreover, the use for nails guarantees reference landmarks with equal and spherical variance, and the location of the nails was uncorrelated (Richtsmeier et al. 2005). Based on this protocol, the intra-observer measurement error, the method-induced measurement error and the inter-observer measurement error were evaluated.

To test the intra-observer measurement error, the exterior surface of the femoral neck of the six left femora was acquired six times, using the MicroScribe, by the first observer. The five reference nails were digitised in the centre of their head at each acquisition. For each femur, the six acquisitions were superimposed using the reference nails, and three different kinds of regression were applied on the three-dimensional coordinates of the points acquired on the femoral neck. For each model, a mean vector of the six vectors obtained for each femur was calculated. The intra-observer measurement error corresponds to the mean angle between the mean vector and each vector of the six repetitions.

To test the method-induced measurement error, the same six left femora were scanned using a Stereoscan Breuckmann® surface scanner with a precision of ± 20 μm after calibration. Using the software VSG AVISO v.6.1.1 (www.vsg3d.com/), the points of the mesh corresponding to the femoral neck were selected and decimated to obtain 4000 points homogeneously positioned for which three-dimensional coordinates were recorded. Three acquisitions were performed by the first observer on each of the six left femora, and the five reference nails were also recorded at each acquisition. For each femur, the three acquisitions performed using the Breuckmann surface scanner and the six acquisitions on dry bone obtained using the MicroScribe were superimposed using the reference nails. The three different kinds of regression were applied on the three-dimensional coordinates of the points acquired on the femoral neck. The method-induced measurement error corresponds to the angle between the mean vector of the six vectors obtained using the dry femora and the mean vector calculated based on the three repetitions performed using the Breuckmann surface scanner.

To test the inter-observer measurement error, a second observer performed three acquisitions on the same six Breuckmann surface scanners. Using the software AVISO, in between 600 and 800 landmarks were put on the femoral neck surface. For each femur, acquisitions performed by the first and second observers were reoriented in the same space using the nails. The angle between the mean vector obtained by the first observer and the mean vector obtained by the second observer was calculated.

Results obtained in this section permitted to select the best three-dimensional model as the one that had the highest repeatability and lowest error variance associated.

Comparison with traditional two-dimensional measurements

Using the three-dimensional axis obtained based on the best model, two angles, traditionally used for the quantification of the femoral neck orientation, were calculated. In a sample of four left femora, the surface of the full femoral shaft was scanned using the MicroScribe programmed to take three-dimensional coordinates 1 cm apart. These coordinates were used to perform a regression based on the equation of a circular cylinder allowing

us to obtain the three-dimensional orientation of the femoral shaft. The angle between the shaft axis and the femoral neck axis was computed and recorded as the neck–shaft angle. Moreover, the three-dimensional axis was projected in the frontal plane defined by the three points on which the femur rested, i.e. the posterior borders of the femoral condyles and the posterior border of the greater trochanter. The angle between this three-dimensional axis and its projection was computed to obtain the value of the angle of anteversion.

Pictures of the four left femora were performed in both the proximal and frontal views. In the proximal view, femora were put on a smooth and horizontal surface with the posterior aspect of the femoral condyles put on the table, and pictures were made in the axis of the femoral shaft. The femoral neck was maintained parallel to the table during acquisition of frontal views. To limit parallax, a telephoto lens Canon f4.5-5.6L IS USM 100–400 mm fixed on a digital reflex camera (Canon Eos 30D 8.2Mpix) was used. Based on these pictures, different axes were drawn using the software ADOBE PHOTO-SHOP CS (www.adobe.com/).

Pictures acquired in proximal views were used to measure the angle of anteversion, defined as the angle between the femoral neck axis and the horizontal. The neck–shaft angle was measured in frontal views as the angle between the femoral neck axis and the femoral shaft axis. In the two cases, the femoral neck axis was defined as the midline between the two borders of the neck (Kingsley & Olmsted, 1948; Ruwe et al. 1992). Values obtained based on two-dimensional pictures and values obtained based on three-dimensional axes were compared.

The three-dimensional axis of the femoral neck in the general femoral geometry: distance with the centre of the head and the shaft axis

The position of the centre of the femoral head in relation to the axis of the femoral neck was analysed. In the sub-sample of 50 femora (25 right and 25 left), the surface of the femoral head was scanned using the MicroScribe programmed to take three-dimensional coordinates 1 mm apart. These coordinates were used to perform a regression based on the equation of a sphere allowing us to obtain the three-dimensional coordinates of the femoral head centre. The location of the coordinates of the femoral head centre in the coordinate system of the PCA, computed based on the centres of the successive ellipses, was calculated. The minimal distance between the coordinates of the femoral head centre and the first principal component of the PCA (representing the femoral neck axis) was calculated (d1 in Fig. 3).

The minimal distance between the femoral neck axis and the shaft axis was analysed. In the sub-sample of 50 femora (25 right and 25 left), the surface of the full femoral shaft was scanned using the MicroScribe and the three-dimensional orientation of the shaft was computed based on a circular cylindrical regression. The minimal distance between the shaft axis and the femoral neck axis was computed (d2 in Fig. 3). The mean point of this minimal distance was recorded and defined as the point of pseudo-intersection between the two axes (P in Fig. 3).

The length of the femoral neck was calculated as the distance between the point of pseudo-intersection between the femoral neck axis and the shaft axis (P in Fig. 3) and the centre of the femoral neck (O in Fig. 3; Rafferty, 1998). This length was normalised using the centroid size of the eight femoral homologous landmarks presented below.
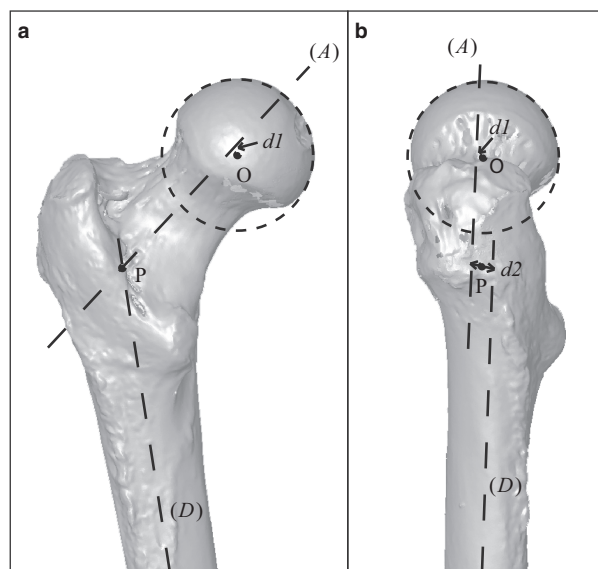
Fig. 3 The position of the three-dimensional axis of the femoral neck was analysed in the general geometry of the femur as illustrated here in a frontal view (A) and a sagittal view (B). Both the distance of the centre of the femoral head and the femoral neck axis (d1), and the distance of the shaft axis and the femoral neck axis (d2) were calculated. (A), femoral neck axis; (D), femoral shaft axis; O, centre of the femoral head; P, pseudo-intersection between the femoral neck axis and the shaft axis.

Applications: study of the three-dimensional orientation of the femoral neck in a sample of modern humans

The three-dimensional orientation of the femoral neck in the full sample of the 91 femora (43 right and 48 left) of modern humans was analysed using the model based on successive cross-sectional ellipses.

During acquisition of the femoral neck surface, eight homologous landmarks were recorded for all femora. These homologous landmarks (presented in Table 1 and Fig. 4) were used to reorient all the femora in the same reference frame. These homologous landmarks were chosen for their minimal observer-induced measurement error. The observer-induced measurement error of these landmarks was computed using the methods of partial superimposition based on reference nails, previously described. A mean measurement error of 1.4 mm was obtained for the eight landmarks with a range of 0.9–1.9 mm. A superimposition based on these true landmarks was performed and the coordinates of the femoral neck surface were passively superimposed. Previously, left femora had been symmetrised to obtain right and left femora in a comparable space. As two separate femora exist as mirror images of each other on the body, a left–right matching symmetry was used. Based on the reoriented coordinates of the femoral neck surface, the orientation of the femoral neck axis was calculated using the model of the successive ellipses.

A vector corresponding to the orientation of the femoral neck for each specimen was thus obtained in a reference space that permits comparisons. It is important to note that, in this approach, the superimposition of the three-dimensional axes of the femoral necks was directly dependent on the inter-individual variation of the

Table 1 List of homologous landmarks used in the study.

No.	Description
1	Pre-trochanteric tubercle, at the level of the iliofemoral ligament attachment
2	Antero-inferior point of the insertion of the *gluteus minimus*
3	Superior-most point of the *pyramidal* muscle attachment
4	Postero-superior point of the posterior inter-trochanteric crest
5	Posterior base of the medial condyle
6	Posterior base of the lateral condyle
7	Maximal of curvature of the trochlea in its central part (frontal view)
8	Maximal of curvature of the distal articular surface between the two condyles
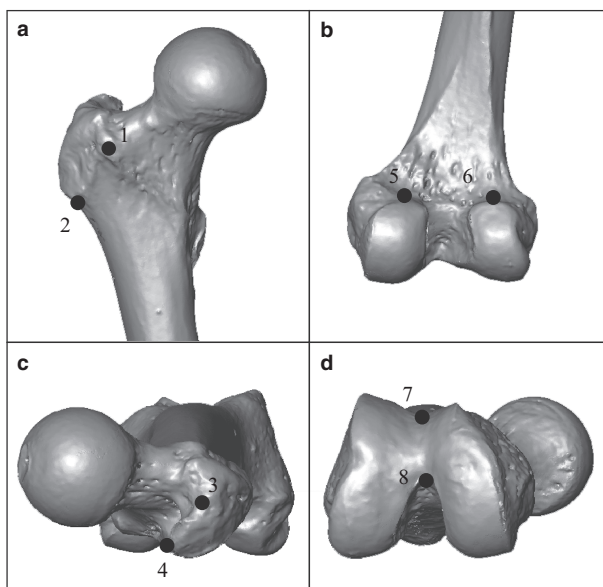
Fig. 4 Homologous landmarks used in the study and further described in Table 1. The scan of the right femur was performed using a Breuckmann® surface scanner. (A) Frontal view of the proximal part; (B) posterior view of the distal part; (C) proximal view; (D) distal view.

landmarks used in the process. Consequently, variation observed in the three-dimensional orientations must always simultaneously be analysed with regard to variations of the shape itself.

A MANCOVA (multivariate analysis of covariance) was performed to test the effect of side (right and left), age (continuous factor based on the log of the age in years), sex (women or men) and size (continuous factor based on the log of the centroid size of the homologous landmarks) on the orientation of the femoral neck. Differences in the orientation of the femoral neck according to the significant factors were explored graphically. Mean vectors between right and left sides of paired femora were computed previously to work on independent data. The vectors of the 50 specimens were used to explore the variability of the orientation of the femoral neck in this sample. A mean vector based on the 50 individ-

ual vectors was computed. An estimation of the variability was obtained using the mean angle between the mean vector and each vector of the 50 specimens.

The influence of inter-individual variation of the homologous landmarks on the superimposition of the femoral neck axes was analysed as well. Tangent space projections of the homologous landmark coordinates were used to compute PCA. A MANCOVA was performed on the non-null principal components to test the effect of side, age, sex and size on the femoral shape. Variation of shape conformation with age was explored using multivariate regression on the non-null principal components. Finally, an ANCOVA (analysis of covariance) was performed to analyse the effects of the different factors on the normalised femoral length.

Results

On the sub-sample of 50 femora, the average deviation computed based on the model using successive cross-sectional ellipses was on average smaller (mean = 0.73 mm; range = 0.51–1.12 mm) than the ones computed based on a single (mean = 1.92 mm; range = 0.93–2.84 mm) or two cylinders (mean = 0.99 mm; range = 0.74–1.41 mm; Fig. 5). According to the ANOVA, the decrease in the average deviation between these three models was significant ($F_{2,147} = 309.9$, $P < 0.001$).

In addition, a decrease in both the intra- and inter-observers measurement errors was observed on the sub-sample of six left femora from the model based on one cylinder to the model based on successive ellipses (Table 2). The method-induced measurement error revealed that there was a negligible difference between measurements obtained based on dry femora and measurements obtained based on Breuckmann surface scans (Table 2). According to these results, it was concluded that the regression based on successive cross-sectional ellipses is more accurate to model the femoral neck.

Do the centres of the successive ellipses represent a unique axis? Considering the sub-sample of 50 femora, the first principal component of the PCA, computed on the centre of the successive ellipses, represented on average 99.8% of the variance, while the PC2 and PC3 represented 0.2 and 0.002%, respectively. The centres of the successive ellipses were thus aligned in a unique axis that is used to represent the femoral neck axis.

The three-dimensional axis obtained using the successive cross-sectional ellipses model was used to compute two traditional angles, the angle of anteversion and the neck–shaft angle, on the sub-sample of four femora. Comparison with values obtained based on traditional methods demonstrates a good correspondence between two-dimensional and three-dimensional methods. Mean differences of 2.4 ° (range = 0.2–5.1 °) and 4.5 ° (range = 2.4–6.0 °) were obtained for the angle of anteversion and the neck–shaft angle, respectively.

On the sub-sample of 50 femora the position of the centre of the femoral head is placed on average very close to
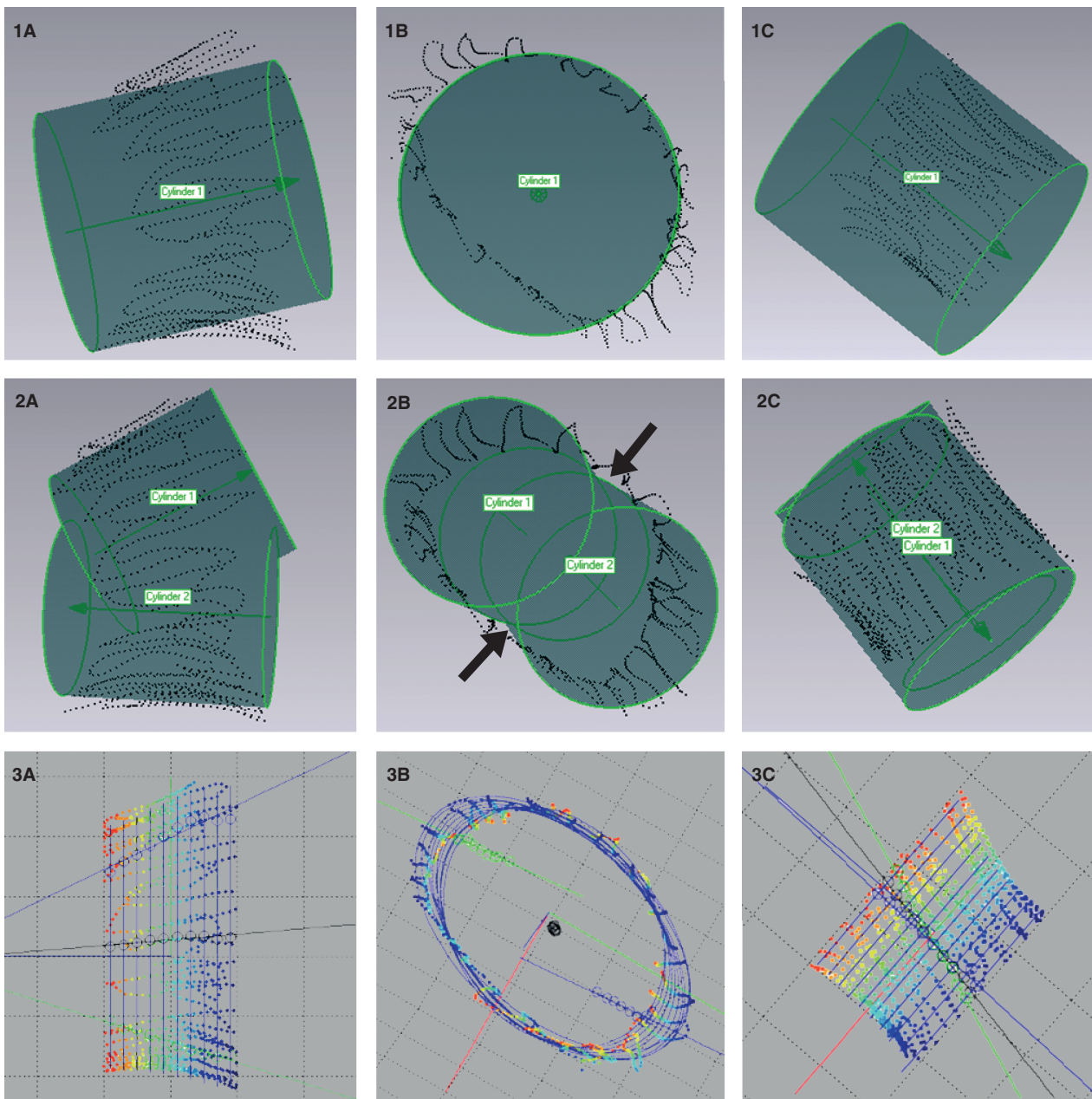
Fig. 5 Results of the three different regression approaches are presented in the frontal (A), transverse (B) and proximal (C) views of the femoral neck. The femoral neck is poorly modelled by a circular cylinder (1): this model overestimates the antero-posterior diameter of the femoral neck. The regression based on two cylinders (2) has the advantage to consider the antero-posterior flattening of the neck and provides a more realistic model. However, an artefact between the two cylinders is created at the intersection of the two surfaces (arrows). Moreover, during the processing, the selection of the anterior and posterior parts of the femoral neck has to be done manually and, thus, involves the intervention of an operator. With the model based on successive cross-sectional ellipses (3), the artefact formed by the two surfaces is absent and the antero-posterior flattening is accurately modelled due to the long axis of the ellipses oriented in the supero-inferior direction of the neck. Moreover, this model considers the antero-posterior narrowing at the middle of the femoral neck, which is ignored by the two other models. Thus, the structure of the femoral neck was better described by the model based on successive cross-sectional ellipses.

the axis of the femoral neck. The mean distance between the femoral head centre and the axis of the femoral neck (d1 in Fig. 3) is 2.5 mm (range = 0.4–5.5 mm). The distance between the femoral neck axis and the femoral shaft axis (d2 in Fig. 3) equals 4.9 mm on average (SD = 2.6 mm; range = 0.01–9.8 mm).

Considering the full sample of 91 femora there is a great variability in the three-dimensional orientation of

the human femoral neck. An average deviation of 6.7 ° compared with the mean vector was obtained. A maximal and minimal deviation of 19.2 ° and 0 °, respectively, was calculated.

There is a significant effect of sex on the orientation of the femoral neck axis (Table 3), while no significant effect was detected on the femoral shape ($P = 0.18$). The anteversion of the femoral neck tends to be greater in women than in men, while no difference was observed in the inclination of the femoral neck (Fig. 6).

A weak but significant effect of age was detected on both the three-dimensional orientation of the femoral neck (Table 3) and the femoral shape ($P = 0.03$). This effect of age on the orientation of the neck was identified as a change due to aging because when the same MANOVA was performed on a sub-sample of the 50 youngest adults, i.e. adults between 18 and 49 years old (mean = 35.9 ± 8.4 years), no significant effect of age was detected ($P = 0.42$). The angle of anteversion tends to decrease with age, while no effect on the inclination was observed (Fig. 6). As illustrated in Fig. 6, the significant difference in shape detected during aging appears in the frontal plane rather than the transverse plane. Thus, an absolute decrease of the angle of anteversion takes place rather than this being an effect of the superimposition process.

No significant effect of laterality and size on the three-dimensional orientation of the femoral neck was detected (Table 3). The same results were obtained if the normalised length of the femoral neck was used as an indicator of the size rather than the centroid size of the homologous landmarks. Thus, there was no change in this orientation of the femoral neck according to the relative length of the neck, as it was sometimes thought (Kapandji, 2007).

Men tend to have a significantly ($F_{1,75} = 7.05$, $P < 0.01$) greater femoral neck length than women. This length was normalised and no size effect was detected, thus the difference in length was a constitutive dimorphism rather than an effect of size difference between men and women.

Discussion

According to our results, the femoral neck is poorly modelled by a circular cylinder, in spite of its intuitive appeal. This model overestimates the antero-posterior diameter of the femoral neck. The complex architecture of the femoral neck, illustrated in Fig. 1b, clearly requires a more complex model. The regression based on two cylinders has the advantage to consider the antero-posterior flattening of the neck and provides a more realistic model. However, an artefact between the two cylinders is created at the intersection of the two surfaces (arrows in Fig. 5). Moreover, during the processing, the selection of the anterior and posterior parts of the femoral neck has to be done manually and, thus, involves the intervention of an operator. With the model based on successive cross-sectional ellipses, the

Table 2 Results of the method- and observer-induced measurement errors.

	One cylinder	Two cylinders	Successive cross-sectional ellipses
Intra	6.0 °	2.7 °	2.0 °
Inter	12.8 °	5.1 °	4.1 °
Method	4.4 °	3.7 °	3.4 °

Table 3 Results of the MANCOVA performed on the three-dimensional orientation of the femoral neck to test the laterality, age, sex and size effects.

	df	Pillai's trace	Approx F	Num df	Den df	PR (> F)
Laterality	1	0.03	0.71	3	73	0.55
Age	1	0.12	3.19	3	73	0.03*
Sex	1	0.21	6.63	3	73	0.0005***
Size	1	0.04	1.13	3	73	0.34
Laterality × age	1	0.02	0.57	3	73	0.64
Laterality × sex	1	0.04	0.93	3	73	0.43
Age × sex	1	0.01	0.36	3	73	0.78
Laterality × size	1	0.01	0.32	3	73	0.81
Age × size	1	0.01	0.19	3	73	0.91
Sex × size	1	0.08	2.02	3	73	0.12
Laterality × age × sex	1	0.02	0.62	3	73	0.60
Laterality × age × size	1	0.02	0.50	3	73	0.68
Laterality × sex × size	1	0.01	0.35	3	73	0.79
Age × sex × size	1	0.02	0.54	3	73	0.65
Laterality × age × sex × size	1	0.05	1.30	3	73	0.28
Residuals	75					

Significance levels: NS, not significant; *significant at 0.05; **significant at 0.01; ***significant at 0.001.
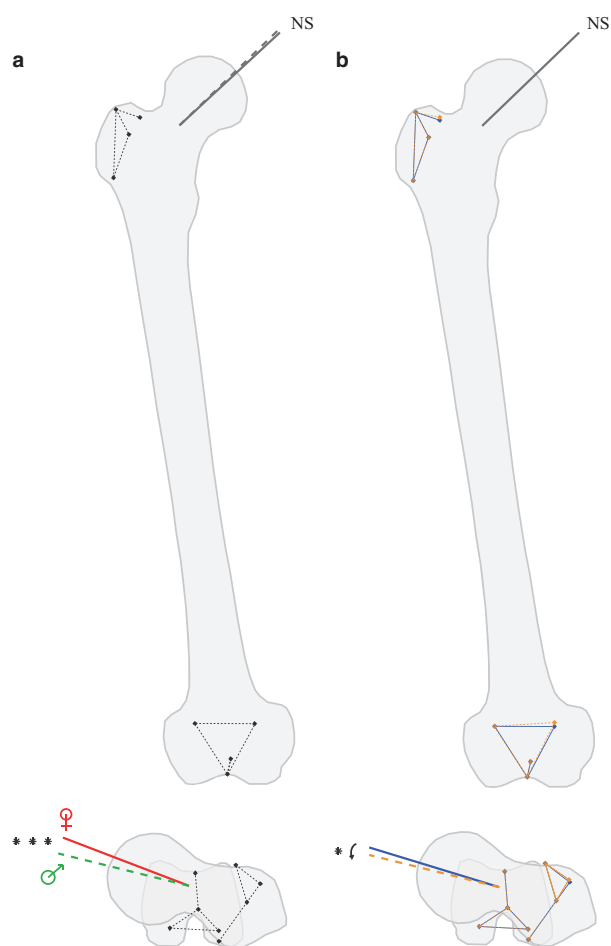
Fig. 6 Significant variations in both the three-dimensional orientation of the femoral neck and the femoral shape are illustrated in colour. (A) A significant difference in the orientation of the femoral neck between men (in dotted lines) and women (in solid lines) was detected. In the transverse plane, the anteversion of the femoral neck tends to be greater in women than in men, while in the frontal plane no difference was observed on the inclination of the femoral neck. No significant effect of sex was detected on the femoral shape and, thus, the mean shape conformation is illustrated. (B) The angle of anteversion tends to decrease with age. Orange dotted lines illustrate changes with age in both the shape conformation and the three-dimensional orientation of the femoral neck compared with the mean shape conformation as illustrated in blue solid lines.

previous artefact is absent and the antero-posterior flattening is accurately modelled due to the long axis of the ellipses oriented in the supero-inferior direction of the neck. Moreover, this model takes into account the antero-posterior narrowing at the middle of the femoral neck that is ignored by the two other models. This narrowing would also be ignored by an elliptic cylinder or an elliptic cone, two models not tested in this study. Thus, the structure of the femoral neck was better described with a complex model that resulted in a decrease of the average deviation from the model based on one cylinder to the model based on successive cross-sectional ellipses. In addition, the

different error measurements performed to evaluate the three-dimensional axis obtained using the successive ellipses demonstrate a great reliability of the process, including data acquisition and data processing. The good alignment of the successive centres of the different ellipses also provides support for this method. In summary, the comparison between the three models indicates that the semi-automatic determination of the three-dimensional axis of the femoral neck based on the model using successive cross-sectional ellipses gives the best description of the actual shape.

The advantage of the three-dimensional method is that any traditional angles can be recalculated on the condition that landmarks defining the given reference plane were digitised during data acquisition. In this study, comparisons of data obtained based on traditional angles and data obtained based on the three-dimensional axis provided evidence that these results are in agreement. Indeed, mean differences of 2.4 ° and 4.5 ° compared with the mean values of the angle of anteversion and the neck–shaft angle, respectively, of 17 ° and 128 ° on the sub-sample of the four femora were considered acceptable.

In addition, the position of the three-dimensional axis of the femoral neck in relation to the centre of the femoral head and the shaft axis provides evidence that the computed axis is biologically meaningful. However, the present results fail to support the results obtained by Kingsley & Olmsted (1948) according to which the femoral head is not centred on the femoral neck axis; although the complex biomechanics of the proximal femur (Pauwels, 1935, 1954, 1980; Inman, 1947; Merchant, 1965; McLeish & Charnley, 1970; Heimkes et al. 1993; Fabeck et al. 2002; Skuban et al. 2009) suggest a complex organisation of the structure that is in accordance with, on the one hand, the location of the centre of the femoral head on the femoral neck axis and, on the other hand, the crossing of the femoral neck axis with the shaft axis.

Finally, variations of the three-dimensional orientation of the femoral neck in a sample of 91 femora were analysed to compare results obtained with the method based on the successive cross-sectional ellipses with data available in the literature.

The three-dimensional orientation of the femoral neck shows a large variation with regard to the homogeneity of the studied sample. Analyses were performed here on European skeletons (French and Swiss), which lived in a modern industrialised society. And yet, the habitual biomechanical loads on the skeleton, reflecting the habitual activities and the life style of human populations, during infancy is known to impact both speed and orientation of growth (Carter et al. 1996; Frost, 2004; Ruff et al. 2006). The level and kind of activity change according to the geo-economical environment of children can play a role in the final orientation of the femoral neck (Anderson & Trinkaus, 1998). Consequently, it would be interesting to analyse the

three-dimensional orientation of the femoral neck across human populations, including skeletons of individuals from different geographical origins that practise different habitual activities in different environments, and present or past skeletons compared with nomadic, sedentary or industrialised behaviours.

In the present sample of 91 femora, no significant difference in the three-dimensional orientation of the right and left femoral necks was detected. Some authors show a difference between right and left sides (e.g. Kingsley & Olmsted, 1948), while others obtain no difference (e.g. Strecker et al. 1997; Anderson & Trinkaus, 1998). Thus, no conclusion in the concordance between present results and the current literature can be established on this point.

A very significant sexual dimorphism in the three-dimensional orientation of the femoral neck was observed. In a superior view, the femoral neck orientation of women tends to be more anteversed (Fig. 6), as it was already observed in the literature (Parsons, 1914; Kingsley & Olmsted, 1948; Yoshioka et al. 1987). No significant effect of size was detected when the size difference between sexes was eliminated. No difference in the orientation of the femoral neck was observed in our sample between small and tall individuals. There is also no interaction between sex and size. Change between sex was due here to intrinsic difference rather than to size difference.

During growth, many changes in the orientation of the femoral neck were observed (Mikulicz, 1878; Le Damany, 1903; von Lanz, 1951; Dunlap et al. 1953; Shands & Steele, 1958; Tardieu & Preuschoft, 1996; Fabeck et al. 2002; Tardieu, 2010; Bonneau et al. 2011). According to our results, there is no change in the three-dimensional orientation of the femoral neck after completion of growth, as it was noted in the literature (Reikeras & Hoiseth, 1982). However, in the transverse view, the orientation of the femoral neck tends to shows a decrease anteversion during aging (after 50 years old), which is in accordance with age-related changes already observed in the internal architecture of the femoral neck (Walker & Lovejoy, 1985), resulting in a geometric restructuration by increasing the breadth of the neck cross-section in men (Beck et al. 1992).

In summary, results obtained here after application of the semi-automatic method developed in this study are in agreement with data available in the literature.

In conclusion, the method to determine the three-dimensional axis of the femoral neck using the model based on successive cross-sectional ellipses proposed in this study is validated by our results. The axis as obtained allows a description of the orientation of the femoral neck in the full three special dimensions. Based on this three-dimensional axis, the traditional angles can be calculated and used in their current applications. It is evident that in many applications a three-dimensional axis cannot be used directly and, as such, the conversion to traditional angles remains useful.

Moreover, the development of this method responded to the difficulty in identifying the true axis of the femoral neck due to its complex architecture. As the model is based on anatomical observations, the computed axis takes into account the complex three-dimensional architecture of the femoral neck and thus provided a true functional axis. In addition, this method is semi-automatic and increases the objectivity of data processing, as after data acquisition the three-dimensional orientation of the neck was determined purely by computation.

The true three-dimensional axis can be compared between individuals based on geometric morphometric tools, here used in order to avoid the reference plane problem. Indeed, a superimposition of the femora based on a reference plane ignores the inter-individual variation of the landmarks used to compute the plane. For example, when the angle of anteversion of the femoral neck was measured, variation in both the posterior aspect of the femoral condyles and the orientation of the lesser trochanter influence the position of the femur in the space and, consequently, the measurement. In this study, femora were superimposed in a three-dimensional reference space rather than a two-dimensional reference plane. The advantages of the superimposition based on homologous three-dimensional landmarks are, firstly, that variation is distributed among all points, which renders the superimposition more objective, and, secondly, that variation in the homologous landmarks can be quantified and used in statistical tests.

Another advantage is that this method can be applied based on different sources: dry bones as used here; but also three-dimensional data obtained based on scanner data (e.g. medical CT-scans). Moreover, the great flexibility of the model, which appears relevant for circular or elliptical cylinders as well as for circular or elliptical cones, could be exploited to generalise the method to other extant and extinct taxa (e.g. non-human hominoids).

Acknowledgements

References

Anderson JY, Trinkaus E (1998) Patterns of sexual, bilateral and interpopulational variation in human femoral neck-shaft angles. *J Anat* **192**, 279–285.

Baylac M (2010) Rmorph a morphometric library for R. Available from the author: baylac(at)mnhn.fr [accessed 1 January 2010].

Beck TJ, Ruff CB, Scott WW, et al. (1992) Sex differences in geometry of the femoral neck with aging: a structural analysis of bone mineral data. *Calcif Tiss Intl* **50**, 24–29.

Bonneau N, Simonis C, Seringe R, et al. (2011) Study of femoral torsion during prenatal growth: interpretation associated with the effects of intrauterine pressure. *Am J Phys Anthropol* **145**, 438–445.

Bookstein FL (1991) *Morphometric Tools for Landmark Data (Geometry and Biology)*. Cambridge: Cambridge University Press.

Braten M, Terjesen T, Rossvoll I (1992) Femoral anteversion in normal adults. Ultrasound measurements in 50 men and 50 women. *Acta Orthop Scand* **63**, 29–32.

Carter DR, van der Meulen MCH, Beaupré GS (1996) Mechanical factors in bone growth and development. *Bone* **18**, 5S–10S.

von Cramon-Taubadel N, Frazier BC, Lahr MM (2007) The problem of assessing landmark error in geometric morphometrics: theory, methods, and modifications. *Am J Phys Anthropol* **134**, 24–35.

Deghrar A, Ruis A, Doursounlan L, et al. (1997) The real measurement of anteversion of the femoral neck by computed tomography (CT scan). *Eur J Orthop Surg Traumatol* **7**, 277–280.

Delialioglu MO, Tasbas BA, Bayrakci K, et al. (2006) Alternative reliable techniques in femoral torsion measurement. *J Pediatr Orthop B* **15**, 28–33.

Dryden IL, Mardia KV (1998) *Statistical Shape Analysis*. New York: Wiley.

Duda GN, Brand D, Freitag S, et al. (1996) Variability of femoral muscle attachments. *J Biomech* **29**, 1185–1190.

Dunlap K, Shanfabeckds AR, Hollister LC, et al. (1953) A new method for determination of torsion of the femur. *J Bone Joint Surg Am* **35**, 289–311.

Durham HA (1915) Anteversion of the femoral neck in the normal femur and its relation to congenital dislocation of the hip. *J Am Med Assoc* **65**, 223–224.

Fabeck L, Tolley M, Rooze M, et al. (2002) Theoretical study of the decrease in the femoral neck anteversion during growth. *Cell Tissues Organs* **171**, 269–275.

Frost HM (2004) A 2003 update of bone physiology and Wolff's law for clinicians. *Angle Orthod* **74**, 3–15.

Gower JC (1975) Generalized Procrustes analysis. *Psychometrika* **40**, 33–50.

Haspl M, Bilic R (1996) Assessment of femoral neck-shaft and antetorsion angles. *Int Orthop* **20**, 363–366.

Heimkes B, Posel P, Plitz W, et al. (1993) Forces acting on the juvenile hip joint in the one-legged stance. *J Pediatr Orthop* **13**, 431–436.

Inman VT (1947) Functional aspects of the abductor muscles of the hip. *J Bone Joint Surg* **29**, 607–619.

Kapandji AI (2007) *Physiologie articulaire Tome 3 Rachis – Ceinture pelvienne – Rachis lombal – Rachis dorsal – Rachis cervical – Tête*, 6th edn. Paris: Maloine.

Kim JS, Park TS, Park SB, et al. (2000a) Measurement of femoral neck anteversion in 3D. Part 1: 3D imaging method. *Med Biol Engng Comput* **38**, 603–609.

Kim JS, Park TS, Park SB, et al. (2000b) Measurement of femoral neck anteversion in 3D. Part 2: 3D modelling method. *Med Biol Engng Comput* **38**, 610–616.

Kingsley PC, Olmsted KL (1948) A study to determine the angle of anteversion of the neck of the femur. *J Bone Joint Surg Am* **30**, 745–751.

Klein P, Sommerfeld P (2008) *Biomécanique des Membres Inférieures. Bases et Concepts, Bassin, Membres Inférieurs*. Paris: Elsevier Masson.

von Lanz T (1951) Über umwelige entwicklungen am menschlichen hüftgelenk. *Schweizerische medizinische wochenschrift* **81**, 1053–1056.

Le Damany P (1903) Les torsions osseuses: leur rôle dans la transformation des membres. *J Anat Physiol* **39**, 126–165, 313–337, 426–450, 536–545.

Lovejoy CO (1988) Evolution of human walking. *Sci Am* **259**, 118–125.

Lovejoy CO (2005) The natural history of human gait and posture. Part 2: hip and thigh. *Gait posture* **21**, 113–124.

Magilligan DJ (1956) Calculation of the angle of anteversion by means of horizontal lateral roentgenography. *J Bone Joint Surg Am* **38**, 1231–1246.

Matsumura A, Gunji H, Takahashi Y, et al. (2010) Cross-sectional morphology of the femoral neck of wild chimpanzees. *Int J Primatol* **31**, 219–238.

McLeish RD, Charnley J (1970) Abduction forces in the one-legged stance. *J Biomech* **3**, 191–209.

Merchant AC (1965) Hip abductor muscle force: a experimental study of the influence of hip position with particular reference to rotation. *J Bone Joint Surg* **47**, 462–476.

Mikulicz J (1878) Ueber individuelle formdifferenzen am femur and an der tibia des menschen. Mit Berücksichtigung der statik des kniegelenks. *Archiv Anat Entwickelungsgeschichte* **117**, 351–407.

Moulton A, Upadhyay SS (1982) A direct method of measuring femoral anteversion using ultrasound. *J Bone Joint Surg Br* **64**, 469–472.

Murphy SB, Simon SR, Kijewski PK, et al. (1987) Femoral anteversion. *J Bone Joint Surg Am* **69**, 1169–1176.

Ohman JC, Krochta TJ, Lovejoy CO, et al. (1997) Cortical bone distribution in the femoral neck of hominoids: implications for the locomotion of Australopithecus afarensis. *Am J Phys Anthropol* **104**, 117–131.

Parsons FG (1914) The characters of the English thigh bone. *J Anat Physiol* **48**, 238–267.

Pauwels F (1935) Der Schenkelhalsbruch – Ein mechanisches Problem – Grundlagen des Heilungsvorganges. Prognose und kausale Therapie. *Z Orthop Chir Suppl* **63**, 38–43.

Pauwels F (1954) Über die verteilung der spongiosadichte im coxalen femurende und ihre bedeutung für die lehre vom funktionellen bau des knochens. Siebenter beitrag zur funktionellen anatomie und kausalen morphologie des stützapparates. *Morph Jb* **95**, 35–54.

Pauwels F (1980) *Biomechanics of the Locomotor Apparatus: Contributions on the Functional Anatomy of the Locomotor Apparatus*. New York: Springer.

Perréard Lopreno G, Eades S (2003) Une démarche actualiste en paléoanthropologie: la collection de squelettes de référence. In: *ConstellaSion. Hommage à Alain Gallay*, Vol. 95. (eds Besse M, Stahl Gretsch LI, Curdy P), pp. 463–472. Lausanne: Cahiers d'Archéologie romande.

R Development Core Team (2011) R: A Language and Environment for Statistical Computing. Vienna, Austria: R Foundation

for Statistical Computing. ISBN 3-900051-07-0, URL http://www.R-project.org/.

Rafferty KL (1998) Structural design of the femoral neck in primates. *J Hum Evol* **34**, 361–383.

Reikeras O, Hoiseth A (1982) Femoral neck angles in osteoarthritis of the hip. *Acta Orthop Scand* **53**, 781–784.

Richtsmeier JT, Lele SR, Cole TM (2005) Landmark morphometrics and the analysis of variation. In: *Variation*. (eds Hallgrimsson B, Hall BK), pp. 49–68. Boston: Elsevier Academic Press.

Rippstein J (1955) Zur Bestimmung der antetorsion des schenkelhalses mittels zweier röntgenaufnahmen. *Z Orthop* **86**, 345–360.

Rogers SP (1931) A method for determining the angle of torsion of the neck of the femur. *J Bone Joint Surg Am* **13**, 821–824.

Rohlf FJ, Slice DE (1990) Extensions of the Procrustes method for the optimal superimposition of landmarks. *Syst Zool* **39**, 40–59.

Ruff C, Holt B, Trinkaus E (2006) Who's afraid of big bad Wolff?: "Wolff's law" and bone functional adaptation. *Am J Phys Anthropol* **129**, 484–498.

Ruwe PA, Gage JR, Ozonoff MB, et al. (1992) Clinical determination of femoral anteversion. A comparison with established techniques. *J Bone Joint Surg Am* **74**, 820–830.

Ryder CT, Crane L (1953) Measuring femoral anteversion: the problem and a method. *J Bone Joint Surg Am* **35**, 321–328.

Seeman E, Duan Y, Fong C, et al. (2001) Fracture site-specific deficits in bone size and volumetric density in men with spine or hip fractures. *J Bone Miner Res* **16**, 120–127.

Shands AR, Steele MK (1958) Torsion of the femur: a follow-up report on the use of the Dunlap Method for its determination. *J Bone Joint Surg Am* **40**, 803–816.

Siffert RS (1981) Patters of deformity on the developing hip. *Clin Orthop* **160**, 14–29.

Skuban TP, Vogel T, Baur-Mlelnyk A, et al. (2009) Function-orientation structural analysis of the proximal human femur. *Cell Tissues Organs* **190**, 247–255.

Slice DE (2005) *Modern Morphometrics in Physical Anthropology*. New York: Kluwer Academic.

Staheli LT, Corbett M, Wyss C, et al. (1985) Lower-extremity rotational problems in children. Normal values to guide management. *J Bone Joint Surg Am* **67**, 39–47.

Strecker W, Keppler P, Gebhard F, et al. (1997) Length and torsion of the lower limb. *J Bone Joint Surg Br* **79**, 1019–1023.

Tamari K, Tinley P, Briffa K, et al. (2005) Validity and reliability of existing and modified clinical methods of measuring femoral and tibiofibular torsion in healthy subjects: use of different reference axes may improve reliability. *Clin Anat* **18**, 46–55.

Tardieu C (2010) Development of the human hind limb and its importance for the evolution of bipedalism. *Evol Anthropol* **19**, 174–186.

Tardieu C, Preuschoft H (1996) Ontogeny of the knee joint in humans, great apes and fossil hominids: pelvi-femoral relationships during postnatal growth in humans. *Folia Primatol* **66**, 68–81.

Tayton E (2007) Femoral anteversion. A necessary angle or an evolutionary vestige?. *J Bone Joint Surg Br* **89**, 1283–1288.

Tönnis D, Heinecke A (1999) Acetabular and femoral anteversion: relationship with osteoarthritis of the hip. *J Bone Joint Surg Am* **81**, 1747–1770.

Walker RA, Lovejoy CO (1985) Radiographic changes in the clavicle and proximal femur and their use in the determination of skeletal age at death. *Am J Phys Anthropol* **68**, 67–78.

Wedge JH, Munkacsi I, Loback D (1989) Anteversion of the femur and idiopathic osteoarthrosis of the hip. *J Bone Joint Surg Am* **71**, 1040–1043.

Wolff J (1892) *Das Gesetz der Transformation der KNOCHEN*. Berlin: August Hirschwald.

Yoshioka Y, Siu D, Cooke TD (1987) The anatomy and functional axes of the femur. *J Bone Joint Surg* **69**, 873–880.

Zebaze RMD, Jones A, Welsh F, et al. (2005) Femoral neck shape and the spatial distribution of its mineral mass varies with its size: clinical and biomechanical implications. *Bone* **37**, 243–252.